**Biogeosciences
Discussions**

Remote sensing the dynamics of suspended particles in the Mackenzie River plume (Canadian Arctic Ocean)

D. Doxaran[1], J. Ehn[1,*], S. Bélanger[2], A. Matsuoka[3], S. Hooker[4], and M. Babin[3]

[1]Laboratoire d'Océanographie de Villefranche, UMR 7093, CNRS-UPMC, France
[2]Université du Québec à Rimouski, Canada
[3]Takuvik Research Unit, Université Laval, Québec, Canada
[4]NASA/GSFC/Code 616.2, Greenbelt, MD 20771, USA
[*]now at: Centre for Earth Observation Science, University of Manitoba, Manitoba, Canada

Abstract

Climate change significantly impacts Arctic shelf regions in terms of air temperature, ultraviolet radiation, melting of sea ice, precipitation, thawing of permafrost and coastal erosion. A direct consequence is an increase in Arctic river discharge with an expectation of increased delivery of organic carbon sequestered in high-latitute soils since the last glacial maximum. Monitoring the fluxes and fate of this terrigenous organic carbon is problematic in such sparsely populated regions unless remote sensing techniques can be developed to an operational stage.

The main objective of this study is to develop an ocean colour algorithm to operationally monitor dynamics of suspended particulate matter (SPM) on the Mackenzie River continental shelf (Canadian Arctic Ocean) using satellite imagery. The water optical properties are documented across the study area and related to concentrations of SPM and particulate organic carbon (POC). Robust SPM and POC:SPM proxies are identified, such as the light backscattering and attenuation coefficients, and relationships are established between these optical and biogeochemical parameters. Following a semi-analytical approach, a regional SPM quantification relationship is obtained for the inversion of the water reflectance signal into SPM concentration. This relationship is validated based on independent field optical measurements. It is successfully applied to a selection of MODIS satellite data which allow estimating fluxes at the river mouth and monitoring the extension and dynamics of the Mackenzie River surface plume in 2009, 2010 and 2011. Good agreement is obtained with field observations representative of the whole water column in the river delta zone within which terrigenous SPM is mainly constrained (out of short periods of maximum river outflow). Most of the seaward export of SPM is observed to occur within the west side of the river mouth.

Future work require the validation of the developed SPM regional algorithm based on match-ups with field measurements, then the routine application to ocean colour

satellite data in order to better estimate the fluxes and fate of SPM and POC delivered by the Mackenzie River to the Arctic Ocean.

1 Introduction

The Arctic Ocean is strongly influenced by direct river inputs (freshwater, nutrients, terrigenous suspended and dissolved substances). Polar amplification of climate change significantly impacts the Arctic Ocean with repercussions on both the regional and global carbon cycles (www.acia.uaf.edu). The melting of ice and permafrost, increasing precipitation and hydrological processes at high latitudes are changing freshwater discharge and the amount of terrestrial organic and inorganic matter that is delivered to the ocean (Peterson et al., 2002; Frey and McClelland, 2009). The fate of the presumably highly refractory terrigenous particulate organic carbon (POC_{ter}), expected to be resistant to degradation in coastal waters until burial in marine sediments, is quite uncertain (Hedges et al., 1997; Shlunz and Schneider, 2000) and warrants careful monitoring in coming years.

The bulk of river discharge into the Arctic Ocean occurs during a relatively short (3–4 months) summer period. During the rest of the year river outflow is greatly reduced by the presence of land-fast ice at the river mouths (McClelland et al., 2012). Monitoring Arctic coastal environments is difficult and costly as they constitute remote sparsely populated areas affected by extreme meteorological conditions. Due to limited field observations of concentrations of terrigenous substances transported by rivers to estuarine zones, current estimates of fluxes delivered by rivers to the Arctic Ocean are associated with dramatic uncertainties which prevent operational monitoring (Schlunz and Schneider, 2000; Lefouest et al., 2011). Ocean colour remote sensing observations represent a great potential for monitoring the fluxes of coloured terrigenous substances delivered by rivers into the Arctic Ocean, i.e. it can be employed to quantify fluxes at monthly, yearly and multi-year temporal scales and detect significant variations induced by changes in Arctic river regimes and draining basins. Such monitoring

requires a calibration of existing ocean colour algorithms to account for the specific inherent optical properties (IOPs) of the coloured suspended and dissolved matters detected within the river mouth and turbid plume areas.

The Malina oceanographic expedition was conducted in the Beaufort Sea (Canadian Arctic ocean) onboard the Canadian research ice-breaker CCGS Amundsen in August 2009 (Fig. 1). The overall goal of the Malina project is to understand how biodiversity and biogeochemical fluxes in the Arctic Ocean are controlled by light penetration and how they are affected by ongoing climate change in the Arctic. The objective of the present study is to develop an algorithm to quantify and monitor the concentrations of suspended particulate matter (SPM) in the Arctic coastal waters directly influenced by the discharge of the Mackenzie River (Canada) and to apply this algorithm to ocean colour satellite data.

The Mackenzie River on its own delivers more terrigenous SPM to the Arctic Ocean than all the other Arctic rivers combined (Rachold et al., 2004; O'Brien et al., 2006), and is the main source of POC_{ter} (Rachold et al., 2004). However, spatial and temporal variations in these fluxes remain poorly documented. The first step is to document the content in organic carbon of SPM exported by the Mackenzie River in the Canadian Beaufort Sea, and then follow the spatial variations of this content along the river plume to the limits of its extension. Taking into account variations of particle composition, a second step is to determine the mass-specific IOPs of the SPM. The results obtained are used to establish a regional SPM quantification relationship for the MODIS ocean colour satellite sensor. This relationship is validated based on coincident field measurements of the water reflectance and SPM concentration, then applied to selected MODIS satellite data to remote sense the dynamics of SPM within surface waters of the Mackenzie River plume. Satellite observations are complemented by field bio-optical measurements carried out in the delta zone to document the dynamics of SPM within the whole water column.

2 Data and methods

2.1 Study area

The southeast of the Beaufort Sea is characterized by the presence of a large continental shelf occupying more than $60\,000\,km^2$, bordered to the east by the Amundsen Gulf, to the west by the Mackenzie Canyon, to the south by the delta of the Mackenzie River, and by the Beaufort Sea and Canada Basin to the north (Fig. 1, Carmack and MacDonald, 2002). North of the Mackenzie Shelf, the circulation is highly variable and often linked to the seasonality of the outflow of the Mackenzie River which discharges $\sim 330\,km^3$ of freshwater within a relatively short temporal window (3–4 months, with a peak at the end of June) (e.g. O'Brien et al., 2006). This discharge typically varies from about $4000\,m^3\,s^{-1}$ during a long winter period (from December to May) to about $25\,000\,m^3\,s^{-1}$ during summer (from June to August) (Fig. 1c).

At the end of winter, thermodynamically grown landfast ice reaches a thickness of approximately 2 m and extends to the 20 m isobath. The external margin of the landfast ice is subject to dynamic interactions with the Arctic pack ice, which results in the formation of ridged ice barrier of considerable thickness ($>20\,m$) (Macdonald et al., 1995). This zone of ice accumulation, known as stamukhi zone, forms a barrier that traps fresh waters from the Mackenzie River. The river water accumulates behind the stamukhi zone during winter and forms what is essentially a lake (unofficially called Lake Herlinveaux) containing approximately $70\,km^3$ of turbid freshwater (Carmack and Macdonald, 2002). Primary production under the landfast ice is weak during this period due to light limitation (solar cycle, ice, intensive vertical mixing).

The spring ice break-up begins with the flooding of the Mackenzie River. By June, river flow is maximal and inundates the coastal zone until the stamukhi gives way under the pressure and melting generated by the warm mass of freshwater collecting upstream. Rapidly, the warm and very turbid plume can extend over an area of several thousand km^2 (Macdonald et al., 1995).

5209

During the summer, melting ice and continual inputs from the Mackenzie River forms a 5 to 10 meters layer of freshwater which occupies the shelf. It should be noted that it is not unusual to find ice above the continental shelf up until the end of July. In September, however, the shelf is typically completely free of ice (up to around $72°\,N$). The movement of the Mackenzie River freshwater plume depends principally on the wind conditions. Under calm or westerly winds, the Coriolis effect tends to maintain the freshwater stream along the coast in an eastward direction, while easterly winds transport the waters offshore towards the Canada Basin (e.g. Macdonald et al., 2002).

2.2 Sampling strategy

A network of sampling stations (Fig. 1) was set to cover the Mackenzie River mouth, delta and continental shelf up to the limit of the Arctic pack ice extent. A total of 74 stations were sampled at least once: (i) using the CTD-rosette from the research icebreaker, (ii) from a barge which was systematically deployed from the ship for bio-optical measurements and (iii) from a Zodiac to collect water in the shallow waters along river transects. Only the barge and Zodiac were used along the river transects stations (Fig. 1b).

At each station, a standard frame comprising a CTD and optical sensors was deployed from the barge using a hand winch and a davit, along vertical profiles from surface to 40 m depth (at 0.2 m per second). Temperature, pressure and salinity were measured using a Seabird Fastcat SBE-49. The optical sensors included: two absorption and attenuation meters (Wetlabs AC9) equipped with 10 and 25 cm long tubes, two backscattering meters (Wetlabs ECO-BB3), one chlorophyll fluorescence sensor (Chelsea) and one CDOM fluorescence sensor (Wetlabs ECO-FL2). Light absorption and attenuation were measured at 14 wavelengths covering the visible and near-infrared spectral regions: 412, 440, 488, 510, 532, 555, 630, 676, 715, 730, 750, 767, 820 and 870 nm. Light backscattering was measured at 6 wavelengths within a similar spectral range (440, 532, 650, 720, 770 and 870 nm).

5210

Apparent optical properties were measured using a Compact-Optical Profiling System (C-OPS) built by Biospherical Instruments Inc. (San Diego, California). The C-OPS system was equipped with an above-water global solar irradiance sensor (E_d) and two in-water downward irradiance and upwelling radiance (E_d and L_u, respectively) sensors. The three radiometers were equipped with the following common 18 optical wavebands: 320, 340, 380, 395, 412, 443, 465, 490, 510, 532, 555, 560, 625, 665, 670, 683, 710, and 780 nm. At each station, C-OPS data were recorded during at least three consecutive downcasts between the sea surface and a variable water depth corresponding to the 1 % light level.

At the end of each cast, water samples were collected from selected depths using Niskin bottles mounted on the CTD-rosette and from surface waters (0.2 m depth) using a water sampling bottle from the barge and Zodiac. Water samples were kept stored in the cold and dark (up to two hours) until returning to the ship for immediate filtration and analyses.

2.3   Biogeochemical measurements

SPM concentration – Known volumes (V, in L) of seawater (0.2 to 6 L, depending on turbidity) were filtered in triplicate through pre-ashed (1 h at 450 °C) and pre-weighed (mass $M0$, in mg) 25 mm glass-fibre filters (Whatman, GF/F 0.7 µm nominal pore size) at low vacuum (Van der Linde, 1998). Each filter was then rinsed with Milli-Q water, dried for 12 h at 60 °C and then stored at −80 °C in a clean Petri dish covered with aluminium foil. In the laboratory, filters were dried for 24 h at 60 °C, prior to weighing under a dry atmosphere (mass $M1$, in mg) to obtain the SPM concentration (in g m^{-3}) as:

$$SPM = (M1 - M0)/V \tag{1}$$

The average coefficient of variation of SPM for triplicates was ±16 %, 10 % and 2 %, respectively for SPM concentrations in the ranges 0.04–1, 1–10 and 10–100 g m^{-3}. The relative uncertainty on measured SPM concentrations was therefore higher for

minimum SPM concentrations, possibly due to: (i) insufficient volume of water filtered, so that the increase in the filter mass ($M1-M0$) was negligible; (ii) increased variability in spatial distributions of particulates in the clearest sampled waters. It was not practical to filter larger volumes of water as filtrations were done until near clogging of the filters. Thus, a reduction in uncertainty would require more replicate sampling, however, this was limited by the volume of water available and the number of filters prepared.

Particulate organic carbon (POC) concentrations were measured on the same GF/F filters used for SPM determination. The filters were acidified with 200–350 µl HCl 2N to remove carbonates, dried at 60 °C overnight and then burned on a precalibrated CHN analyzer (Perkin Elmer 2400, combustion at 925 °C) for determination of the CO$_2$ produced. The average coefficient of variation of POC for triplicates was 11 %, and it was 7 % for the POC:SPM ratio.

2.4   Optical measurements

In this paragraph we describe successively the measurements of the inherent optical properties (IOPs, measured in situ and in laboratory) and apparent optical properties (AOPs, namely the remote sensing reflectance, R_{rs} in sr^{-1}, measured in the field).

CTD-IOP frame – The CTD, absorption, attenuation and fluorescence signals recorded using the instruments carried by the CTD-IOP frame were binned over 1-second periods, which is imposed by the instrument with the lowest acquisition rate, i.e. the ECO-BB3. Taking into account the down and upward speed of the frame, a resulting minimum of 5 measurements were obtained every meter along the water column.

The ac-9 sensors were regularly calibrated using pure (Milli-Q) water, i.e. before, during and after the Malina field campaign. The raw absorption and attenuation spectral values were corrected for temperature and salinity effects following the recommended procedure (Wetlabs ac-9 User'Guide, 2008) using correction coefficients provided by Sullivan et al. (2006) and Langford et al. (2001), respectively, in the visible and near-infrared spectral regions. The "proportional" method was then used to correct for

residual scattering effects on absorption measurements (Zaneveld et al., 1994). Wavelength 870 nm was used as the reference wavelength where particulate absorption was assumed to be negligible.

The total volume scattering function measured at 117° with the ECO-BB3 sensors, β (117°) in $m^{-1}\,sr^{-1}$, was first corrected for absorption losses along the scattered photon pathway (Wetlabs ECO BB User's Guide, 2007). Then, taking into account the measured water temperature, molecular scattering by water was calculated (Morel, 1974) and subtracted from the absorption-corrected values to retrieve the particulate scattering signal, $\beta p(117°)$. Finally, the particulate backscattering coefficient, $b_{bp}(\lambda)$ in m^{-1}, was determined through estimation from $\beta p(117°)$ using the χ factor proposed by Boss and Pegau (2001) based on measurements of the volume scattering function with high angular resolution in a diversity of water types. The different steps in the processing of the ECO-BB data are summarized as:

$$b_{bp}(\lambda) = 2\pi\chi\{\beta(117°, \lambda, a)e^{0.0391a} - \beta_w(117°, \lambda)\} \tag{2}$$

where λ, in nm, is the wavelength; a in m^{-1}, is the absorption coefficient measured with ac-9 sensors at the corresponding wavelength and χ has a fixed value of 1.1.

The particulate scattering coefficient, b_p in m^{-1}, was simply obtained as the difference between the measured attenuation and absorption coefficients:

$$b_p(\lambda) = c(\lambda) - a(\lambda) \tag{3}$$

As a result, the vertical profiles of water temperature, salinity and fully-corrected multi-spectral optical properties (absorption, attenuation, particulate scattering and backscattering coefficients, CDOM and Chl a fluorescence signals) were obtained at each station.

Laboratory measurements – Water samples collected from the barge and Zodiac were transported to the ship for measurements of particulate absorption using the filter-pad technique. A known volume of sampled water was filtered through Whatmann GF/F glass-fibre filters. Each filter was then placed in the centre of a 150 mm

integrating sphere (Labsphere) equipped with a home-made filter-holder (see Röttgers and Gehnke (2012) for technical details). This method does not require near-infrared correction as scattering effects are negligible. The optical density (OD_f) of particles retained on the filter was then measured using a Perkin-Elmer Lambda-19 spectrophotometer, from 300 to 800 nm. OD_f was converted into particulate absorption coefficient (a_p, m^{-1}) using the following expression:

$$a_p = \frac{2.303}{\alpha} \cdot (OD_f - OD_{blank}) \cdot \frac{A}{V} \tag{4}$$

where OD_{blank} is the absorbance of a blank filter, A the clearance area of the particles on the filter (m^2), V the volume filtered (m^3), and α a path length amplification factor. OD_{blank} was determined by averaging the absorbance spectra of 12 blank-filters measured during the course of the field campaign (e.g. $OD_{blank}(550) = -0.005 \pm 0.002$). While α is within the range 2 to 2.5 when OD is determined using the common transmittance technique (Roesler, 1998), it reaches ~4 to ~4.5 when OD is determined using an integrating sphere (Röttgers and Gehnke, 2012). Röttgers and Gehnke (2012) observed a linear relationship between OD_f and a_p, with the condition $OD_f < 0.1$ and recommended a value of 4.5 for α. However, α tends to decrease when OD_f increases beyond 0.1 (Röttgers and Gehnke, 2012). Since it was not always possible to keep $OD_f < 0.1$ due to the large number of samples processed onboard, we adopt the following relationship between α and OD_f derived from batch cultures (Röttgers, personal communication, 2010):

$$\alpha = 2.9OD_f^2 - 4.76OD_f + 4.5 \tag{5}$$

Pigments were then extracted within 24 h, using methanol (Kishino et al., 1985), which essentially removes all pigments (95 % of sample). The filter was once again placed in the centre of the integrating sphere to measure the absorption coefficient of non-algal particles, a_{nap} in m^{-1}. The absorption coefficient of phytoplankton, a_{phy} in m^{-1}, was obtained by subtracting a_{nap} from the total particulate absorption coefficient. For

some exceptions, a_{nap} data were fitted between 300–380, 521–640 and 700–750 nm to eliminate residue of pigment absorption (see Babin et al., 2003a). For a few samples, no a_{nap} data were available and the a_{phy} spectrum was obtained numerically following Bricaud and Stramski (1990).

The detailed methodology to determine the light absorption coefficient of CDOM is described in Matsuoka et al. (2012). Briefly, water samples from the barge and Zodiac were collected using cleaned plastic bucket or glass-bottles and kept stored in the cold and dark until our return to the ship. Water samples were then immediately filtered using 0.2 μm GHP filters (Acrodisc Inc.) to measure light absorbance by CDOM using a liquid waveguide system, UltraPath (World Precision Instruments, Inc.) from 200 to 735 nm at 1 nm increments. This instrument allows selection of the most appropriate optical pathlength ranging from 0.05 to 2 m (i.e. 0.05, 0.1, 0.5 or 2 m). In most cases, a 2 m optical pathlength was used for the measurement, except for coastal waters at the Mackenzie River mouth where a 0.1 m optical pathlength was used. The absorption coefficient of CDOM, a_{CDOM} in m^{-1}, was then calculated (Matsuoka et al., 2012).

In situ AOP measurements – The R_{rs} signal is defined as the ratio between the water-leaving radiance, L_w in $W\,m^{-2}\,sr^{-1}\,nm^{-1}$, and the global solar irradiance signal, E_d in $W\,m^{-2}\,nm^{-1}$, both just above the sea surface at $z=0^+$ (Mobley, 1994). At each station, the L_w and E_d signals were respectively derived and measured using a C-OPS. This instrument is based on a cluster of 19 state-of-the-art microradiometers spanning 320–780 nm and a new kite-shaped backplane design (Morrow et al., 2010) which includes tuneable ballast and buoyancy plus pitch and roll adjustments, to provide unprecedented stability and vertical resolution in near-surface waters. Data sets collected as part of the development activity to produce the first C-OPS instrument and the Malina expedition were of sufficient resolution and quality to show, uncertainties in the execution of apparent optical properties sampling protocols are measurable at the 1 % and 1 cm level with C-OPS (Hooker et al., 2012).

During three consecutive C-OPS downcasts, the upwelling radiance was measured as function of water depth and extrapolated up to the water surface (at null depth $z=0^-$)

over a near-surface interval with homogenous water properties (verified with temperature and attenuation parameters). The water-leaving radiance signal, L_w, was obtained from $L_u(0^-)$ as:

$$L_w(\lambda, 0^+) = 0.54 L_u(\lambda, 0^-), \tag{6}$$

where the constant 0.54 accurately accounts for the partial reflection and transmission of the upwelled radiance through the sea surface, as confirmed by Mobley (1999). A verification of the extrapolation process used to determine $L_u(\lambda, 0^-)$ was provided by comparing the in-water determination of $E_d(\lambda, 0^-)$ to the above-water solar irradiance signal using:

$$E_d(\lambda, 0^-) = 0.97 E_d(\lambda, 0^+), \tag{7}$$

where the constant 0.97 represents the applicable air–sea transmittance, Fresnel reflectances, and the irradiance reflectance, and is determined to an accuracy better than 1 % for solar elevations above 50° and low-to-moderate wind speeds.

The appropriateness of the extrapolation interval was evaluated by determining if (7) was satisfied to within approximately the uncertainty of the calibrations (a few percent); if not, the extrapolation interval was redetermined while keeping the selected depths with a homogeneous layer until the disagreement was minimized (usually to within 5 %).

3 Results and discussion

3.1 Concentration and composition (organic carbon content) of suspended particles

Lack of regular measurements made at the mouth of the Mackenzie River prevents the operational monitoring of the solid (SPM and POC_{ter}) fluxes delivered by the river to

the Arctic Ocean. Based on field data collected episodically more than ten years ago, Yunker et al. (1993) observed an approximately stable SPM content of POC_{ter} at the river mouth ($1.4 \pm 0.2\%$) during spring and summer floods; the annual fluxes of SPM and POC_{ter} have been roughly estimated (Macdonald et al., 1998; O'Brien et al., 2006).

During the Malina field campaign, SPM concentrations within surface waters (0–1 m depth) were observed to vary between 0.05 and $142\,g\,m^{-3}$, with arithmetic and geometric mean values of 2.9 and $0.6\,g\,m^{-3}$, respectively. Suspended particles from the river delta, river plume and from the Beaufort Sea away from direct influence of the river plume could be considered separately and were distinguished based on their SPM concentration range: 10–$150\,g\,m^{-3}$, 1–$10\,g\,m^{-3}$ and 0.05–$1\,g\,m^{-3}$, respectively. The surface POC concentration was observed to vary between 0.01 and $2\,g\,m^{-3}$, with arithmetic and geometric mean values of 0.11 and $0.05\,g\,m^{-3}$, respectively.

Interestingly, linear relationships were found between the SPM and POC concentrations, in each of the water masses (delta, plume and open waters) (Fig. 2). A determination coefficient close to 1 and a slope of 0.0089 were found in the river delta (Fig. 2a), indicating a stable composition of suspended particles (a priori mineral-rich particles, average POC:SPM = 2.2 %). The robustness of this relationship could not be assessed in detail as only two river transects were conducted (west and east river mouths). In the river plume, the determination coefficient of the linear relationship is much lower ($R^2 = 0.51$) indicating higher variations of the SPM composition in this transition zone between mineral-rich particles in turbid river waters and the potentially organic-rich particles in open ocean waters (average POC:SPM = 12.2 %). This last statement is confirmed by a high determination coefficient ($R^2 = 0.85$, average POC:SPM = 21 %) is observed between the SPM and POC concentrations in open ocean waters (probably due to reduced variability in particle composition).

A major implication in terms of operational monitoring is that if surface SPM concentrations can be retrieved from either ocean colour remote sensing or field optical measurements over the study area, the corresponding POC concentration can be reasonably well estimated using the empirical linear relationships presented here (Fig. 2a).

This statement remains valid when considering SPM which were sampled at various water depths from 0 to 150 m, including the deep chlorophyll maximum (Fig. 2b). Compared with results obtained for surface waters, the relationship between SPM and POC within the water column: (i) is the same in the river delta (as only surface waters were sampled); (ii) only slightly changes in the open ocean waters (slope of 0.20 instead of 0.21) with a slight decrease of the determination coefficient (R^2 of 0.79 instead of 0.85). However in the river plume waters, the linear relationship between SPM and POC becomes highly scattered (R^2 of 0.18), most probably due to strong variations in SPM composition.

A simple way to examine the variations of SPM composition in the study area is to use the POC:SPM ratio, expressed in %. In open ocean waters, an average relationship has been observed relating the POC content of marine particles to their mean organic matter composition: SPM_{org}:POC = 2.6 (Copin-Montégut, 1980; Van Raaphorst and Melschaert, 1996, see also Babin et al., 2003b). In the case of organic-rich particles ($SPM \approx SPM_{org}$), the inverse ratio POC:SPM would be equal to 38.5 %, say $40 \pm 5\%$. On the other hand, mineral-rich particles such as suspended sediments delivered by rivers to the ocean are expected to have a low POC:SPM ratio, e.g. between 1 and 2 % in the case of the Mackenzie River (Yunker et al., 1993).

In the Malina dataset (Fig. 3), suspended particles sampled in the river delta present a POC:SPM ratio of $2 \pm 1\%$, with extreme values of 1 and 4 %, which is in close agreement with previous observations of Yunker et al. (1993). Inversely, in open ocean waters, the POC:SPM ratio presents strong variations from 15 to 40 %, indicating that some of the particles sampled in the Beaufort Sea were almost 100 % organic. Again the river plume waters appear as a transition zone where the POC:SPM ratio varies from 5 to 16 %, i.e. from mineral-rich to organic-dominated particles. When considering SPM sampled at all waters depths, maximum POC:SPM ratios are observed (corresponding to almost entirely organic particles in the deep chlorophyll maximum).

3.2 Characterisation of the inherent optical properties

The inherent and apparent optical properties of surface waters in the Mackenzie continental shelf are analyzed in order to establish proxies for the quantification of SPM from in situ and satellite remote sensing measurements. The inherent optical properties which directly impact on the ocean colour remote sensing signal (R_{rs}) are the absorption and backscattering coefficients (e.g. Gordon et al., 1975; Morel and Prieur, 1977). Inherent optical properties commonly used in field measurements for quantifying SPM concentration are the attenuation, and particulate scattering and backscattering coefficients. In this section, only measurements carried out along the river transects and in the most turbid stations of the river plume (SPM > 1 g m^{-3}) are considered, as the objective of the study is to monitor the SPM dynamics in the river mouth and plume areas.

Firstly, consistency between absorption measurements made in situ with ac-9 sensors and in the laboratory with bench spectrophotometers is assessed. As the ac-9 sensor is calibrated using pure water, the measured absorption signal is only representative of the CDOM and SPM contributions. Absorption values measured within the first meter below the water surface (0–1 m depth) were averaged for direct comparison with laboratory absorption measurements on water samples collected at the same water depth. A satisfactory result was obtained when plotting the absorption coefficient from the ac-9 vs. the CDOM absorption coefficient (from the Ultrapath) plus the total particulate absorption coefficient (spectrophotometer equipped the integrating sphere); at 440 nm, a linear relationship is obtained with a slope close to 1 (0.96), a null intercept and determination close to 1 (R^2 = 0.97) (Fig. 4a). A direct implication is that the total particulate absorption coefficient can be retrieved by subtracting the a_{CDOM} signal (Ultrapth) from the absorption coefficient measured with the ac-9 sensors. To determine the SPM-specific absorption coefficient, a_p in m^2 g^{-1}, the measured absorption signal from the ac-9 minus CDOM absorption, i.e. the difference [a_{ac9}–a_{CDOM}], was regressed as a function of SPM concentration. Results obtained at 440 nm (Fig. 4b) show, to a

first approximation, that a unique SPM-specific absorption coefficient can be derived which is representative of the most turbid waters in the Mackenzie River plume and delta.

As the total absorption coefficient is obtained from the inversion of the R_{rs} signal, i.e. from atmospherically-corrected ocean colour satellite data, the next step was to identify spectral bands were the contribution of SPM is predominant over that of CDOM. The inverse exercise (i.e. retrieving the CDOM absorption coefficient from the total absorption signal) was successfully achieved in the Mackenzie River plume by Bélanger et al. (2008). Except at the river mouth where the water optical properties were observed to be SPM-dominated, the CDOM contribution to total absorption proved to be predominant at short visible wavelengths ($\leq$ 550 nm) (Fig. 4c). The before longer wavelengths should be preferably used to avoid a major influence of CDOM.

The respective contributions of phytoplankton pigments and non-algal particles on particulate absorption were then assessed using spectrophotometer measurements on particles retained on glass-fibre filters, before and after bleaching for depigmentation. The spectral variations of the ratio a_{nap}:a_p (Fig. 4d) show as expected that spectral bands centred around the Chl a absorption peaks (440 and 675 nm) should be avoided. The contribution of phytoplankton pigments is minimum (<20 %) in the near-infrared spectral region (>700 nm) but also within a visible spectral window (530–650 nm).

Taking into account the spectral contributions of CDOM and phytoplankton pigments to total absorption, wavebands in the near-infrared and in between 530 and 650 nm should be used to retrieve the SPM concentration in the Mackenzie River plume from R_{rs} measurements.

The next step, in the scope of quantifying SPM from field and remote sensing bio-optical measurements, was to relate the attenuation, particulate scattering and backscattering coefficients to the SPM concentration.

A linear relationship is obtained between c(555) and SPM, with a slope and determination coefficient both close to 1, and a negligible intercept (Fig. 5a). The exact slope (1.01 m^2 g^{-1}) can be used to convert attenuation measurements into SPM

concentrations over the Mackenzie River plume. Note that results are only presented up to SPM concentrations of $20\,\mathrm{g\,m^{-3}}$, as the ac-9 sensors did saturate at the highest SPM concentrations encountered at the river mouth (west side). A linear relationship with null intercept and a determination coefficient close to 1 is obtained between $b_{\mathrm{p}}(555)$ and SPM (Fig. 5b); however the slope ($0.88\,\mathrm{m^2\,g^{-1}}$) is lower than that obtained for $c(555)$, indicating that at 555 nm, light scattering by particles contribute almost 90 % of the total attenuation signal.

Finally a third linear relationship is established between the particulate backscattering coefficient, b_{bp}, and SPM, which is a fundamental relationship for the remote sensing of SPM in the Mackenzie River plume. This linear relationship is obtained at all the considered visible and near-infrared wavebands ($R^2 > 0.94$) with the highest determination coefficients ($R^2 > 0.97$) in the near-infrared spectral region, e.g. at 715 nm (Fig. 5c). Note the value of the SPM-specific backscattering coefficient obtained at 715 nm is slightly higher than values reported by Neukermanns et al. (2012) in the North Sea and French Guyana coastal waters, most probably as our dataset was focused on the mineral-rich particles of the Mackenzie delta zone.

Additionally, the particulate backscattering ratio, $b_{\mathrm{bp}}{:}b_{\mathrm{p}}$ in %, is known to be to some extent representative of the SPM composition. This ratio is typically lower or equal to 1 % in phytoplankton-dominated waters (Twardorski et al., 2001) and higher or equal to 2 % in coastal waters (McKee et al., 2009). The Malina dataset reveals that SPM in the Mackenzie River plume are typically mineral-rich particles specific of so-called Case 2 waters, with a $b_{\mathrm{bp}}{:}b_{\mathrm{p}}$ ratio at 715 nm of 2.2 % (Fig. 5d). This ratio significantly decreases to 1.5 % in the clearest waters sampled offshore the river plume: for $b_{\mathrm{p}}(715)$ $< 0.05\,\mathrm{m^{-1}}$ as mineral-rich SPM turns to be phytoplankton-dominated.

3.3 Ocean colour SPM quantification algorithm

Characterization of the inherent optical properties in waters directly influenced by the Mackenzie River plume has therefore allowed (i) establishment of direct bio-optical

proxies for SPM concentration, namely the attenuation and backscattering coefficients; (ii) identification of the most appropriate spectral bands for remotely sensing SPM using e.g. MODIS or MERIS satellite data.

Taking into account the results obtained (paragraph 3.2), a semi-analytical approach is used to develop a robust SPM quantification relationship for the Mackenzie River plume. Following the approach developed by Doxaran et al. (2006), the spectral R_{rs} signal can be related to the SPM concentration according to:

$$R_{\mathrm{rs}}(\lambda) = \frac{0.176}{Q(\lambda)} \frac{b_b(\lambda)}{a(\lambda) + b_b(\lambda)} \tag{8}$$

with a and b_{b} the total absorption and backscattering coefficients (including the pure water contribution) and Q the ratio of upwelling irradiance to upwelling radiance (to a first approximation, a constant Q value of 3.6 sr was considered).

Note there are currently no agreed look-up tables for the Q factor in turbid coastal waters (but see the simulations made by Loisel and Morel (2001) and Park and Ruddick (2005)). The Q factors measured along river transects during the Malina field campaign, using a miniaturized multispectral (406, 438, 494, 510, 560 and 628 nm) radiance camera (see Antoine et al., 2012, for measurement details), showed very limited spectral variations: maximum variations of 10 % between 406 and 628 nm, 7 % on average, at nadir. While limited to the visible spectral domain, these measurements support the use of a spectrally-flat Q factor in our model. Both a and b_{b} coefficients are the sums of the contributions by the main optically active water constituents: pure seawater (w), CDOM and SPM (p) (which can be subdivided into Chl a, for phytoplankton, and non-algal particles):

$$a(\lambda) = a_{\mathrm{w}}(\lambda) + a_{\mathrm{CDOM}}(\lambda) + SPM \times a_{\mathrm{p}}^{*}(\lambda) \tag{9}$$

$$b_{\mathrm{b}}(\lambda) = b_{\mathrm{bw}}(\lambda) + SPM \times b_{\mathrm{bp}}^{*}(\lambda) \tag{10}$$

where a_p^* and b_{bp}^* are respectively the SPM mass-specific absorption and backscattering coefficients, in $m^2\,g^{-1}$.

In sediment-dominated waters, robust SPM quantification relationships can be established using R_{rs} band ratios between the near-infrared (e.g. $\lambda_{NIR} = 800$ or $850\,nm$) and visible (e.g. $\lambda_{VIS} = 550$ or $650\,nm$) spectral regions (Doxaran et al., 2002, 2003, 2006). As a first approximation, assuming limited spectral variations of bi-directional effects, such a ratio can be written as:

$$\frac{Rrs(\lambda_{NIR})}{Rrs(\lambda_{VIS})} = \frac{b_{bp}(\lambda_{NIR})}{b_{bp}(\lambda_{VIS})} \frac{a_w(\lambda_{VIS}) + a_{CDOM}(\lambda_{VIS}) + SPM \times [a_p^* + b_{bp}^*](\lambda_{VIS})}{a_w(\lambda_{NIR}) + SPM \times [a_p^* + b_{bp}^*](\lambda_{NIR})} \tag{11}$$

where light absorption by CDOM is assumed to be negligible in the near-infrared; the contribution by pure water to light backscattering is also negligible compared to that of SPM (for SPM $>1\,g\,m^{-3}$).

This simple model was run selecting 560 and 780 nm, respectively, as visible and near-infrared wavelengths (as they match available C-OPS bands). The spectral pure water absorption coefficients are taken from Kou et al. (1993). The SPM-specific absorption and backscattering coefficients are set to the mean values documented in the present study: 0.0198 and 0.0031 $m^2\,g^{-1}$ for the mass-specific absorption coefficients at 560 and 780 nm; 0.0187 and 0.0175 $m^2\,g^{-1}$ for the mass-specific backscattering coefficients at 560 and 780 nm. The contribution of CDOM to light absorption is determined based on results reported on Fig. 4c: $[a_p + a_{CDOM}](560) = 1.30 \times a_p(560)$ and $[a_p + a_{CDOM}](780) = 1.05 \times a_p(780)$. The resulting mean relationship obtained between $R_{rs}(780){:}R_{rs}(560)$ (Fig. 6a) is of the same type as those obtained in several European sediment-dominated estuaries, namely the Gironde, Loire and Tamar (Doxaran et al., 2006).

An empirical SPM quantification relationship is obtained by regressing the $R_{rs}(780){:}R_{rs}(560)$ values measured by the C-OPS system as a function of measured SPM concentrations. The results obtained (black points in Fig. 6a) tend to validate the

5223

semi-analytical relationship established using the mean SPM-specific inherent optical properties (grey points in Fig. 6a). Note the semi-analytical model tends to overestimate the lowest SPM concentrations ($\leq 1\,g\,m^{-3}$) where some of the assumptions made in Eq. (9–11) are no longer valid. However a cross-validation is obtained between the empirical and semi-analytical approaches for higher SPM concentrations.

The inverse relationship allows retrieval of the surface SPM concentration in the Mackenzie River mouth and turbid plume from R_{rs} measurements around 560 and 780 nm (Fig. 6b). A second order polynomial equation fits this relationship over the whole range of SPM observed in situ (0.1–150 $g\,m^{-3}$).

We further examine the sensitivity of the mean semi-analytical relationship to the variations in $a_p^*(\lambda)$, $b_{bp}^*(\lambda)$ and the CDOM contribution to total absorption. Successive tests show that the respective influences of a_p^* and b_{bp}^* at 560 and 780 nm are more limited than the influence of a changing contribution of light absorption by CDOM. Based on results reported on Fig. 4c, the ratio $[(a_p + a_{CDOM}) / a_{CDOM}]$ at 560 nm varies from 1.10 to 1.60 around the mean value initially set at 1.30. Taking into account these variations of the CDOM contribution to absorption, the extreme relationships used to retrieve the SPM concentration from the $R_{rs}(780){:}R_{rs}(560)$ ratio can be computed (Fig. 6c), which provide a first estimation of the uncertainties associated with the recovered SPM concentration.

3.4 Remote sensing of SPM dynamics in the Mackenzie River plume

The next step is to apply the obtained SPM quantification relationship to ocean colour images. MODIS-Aqua satellite data were selected in this study because of their (i) temporal resolution (at least one image recorded every day, depending on cloud cover), (ii) spectral resolution (providing one waveband at 555 nm and one at 748 nm, i.e. close to those required: 560 and 780 nm) and (iii) availability of several bands in the near-infrared and short-wave infrared spectral regions, which are useful for atmospheric corrections over turbid coastal waters (Wang and Shi, 2007).

5224

MODIS-scenes were selected in 2009, 2010 and 2011 to provide a synoptic view of the seasonal to multi-annual dynamics of SPM in the Mackenzie River plume. The selected dates are: 26 July, 31 July and 21 August 2009 (the 2009 summer period when the Malina campaign took place was associated with high cloud coverage); 4 August, 17 August and 7 September 2010; 28 June, 26 August and 12 September 2011. Two multi-scattering atmospheric corrections methods were tested on the selected MODIS data: (i) the near-infrared correction (two bands) suitable for the case of moderately turbid waters and (ii) the near-infrared/shortwave-infrared switching method better adapted to highly turbid waters (Wang and Shi, 2007). The first correction proved to be suitable for the majority of the turbid waters of the Mackenzie River plume with only the most turbid waters located at the river mouth being sometimes flagged. The second correction produced very similar results as the switch to shortwave-infrared wavelengths was only required for a few pixels corresponding to the most turbid waters at the river mouth. The first correction method was thus selected to retrieve the R_{rs} signal at 555 and 748 nm, compute the $R_{rs}(780):R_{rs}(560)$ ratio and finally apply the mean SPM quantification relationship (Fig. 6b). Clouds and sea-ice were systematically flagged. Results proved to be satisfactory in terms of retrieved ranges of $R_{rs}(780):R_{rs}(560)$ values and SPM concentrations (Fig. 7).

Only the summer period (June–September) is suitable for ocean colour satellite observations of the Mackenzie River plume due to limits imposed by solar light availability and sea-ice cover. However this short period represents most of the variability observed in the region, such as the breaking-up of the stamukhi (natural ice barrier at the river mouth), development and offshore extension of the Mackenzie turbid waters over the continental shelf and the progressive settling of the SPM on the shelf which depends mainly on wind, tides, sea-ice and regional circulation conditions.

Very few cloud-free images were recorded coincidently with the Malina field experiment, i.e. between June and August 2009 (Fig. 1c). SPM maps derived from MODIS-Aqua data at the end of July show high SPM concentrations (from 10 to 50 g m^{-3}) extending 200 km offshore from the river mouth (Fig. 7). SPM tended to be transported

westwards, following the bottom morphology to the Mackenzie Canyon. One month later, at the end of August, the extension of the plume was more limited and SPM were clearly concentrated around the river mouth, resulting in the development of a maximum turbidity zone along the west side of the delta. The progressive decrease of freshwater river discharge in June (23 900 m^3 s^{-1}), July (20 200 m^3 s^{-1}), and then August to September (13 300 and 14 400 m^3 s^{-1}, respectively, see Fig. 1c) explains the observed variation of SPM concentrations.

On the 4 August 2010, high SPM concentrations were located at a maximum turbidity zone in the river delta, as in August 2009. Thirteen days later (17 August 2010), the river plume was extending north with SPM concentrations higher than 10 g m^{-3} observed 250 km offshore (Fig. 7). A similar plume extension could be observed three weeks later (7 September 2010) but now with slightly lower SPM concentrations and a plume extending 200 km offshore (instead of 250 km mid-August). These SPM dynamics may be explained by peculiar variations of the river discharge during the summer 2010. The outflow reached its annual maximum in May (17 700 m^3 s^{-1}), significantly decreased in June (14 000 m^3 s^{-1}) then increased again and remained approximately stable in July and August (15 700 m^3 s^{-1}) (Fig. 1c).

In 2011, one cloud-free image offered a view of the extension of the river plume at the end of June (Figs. 1c and 7). At this time the offshore extension was the largest observed and corresponded to the highest surface SPM concentrations retrieved along the continental shelf, mainly along a channel from the west river mouth to the Mackenzie Canyon. This situation most probably resulted from the recent breaking of the stamukhi. The next available cloud-free images, measured at the end of August and beginning of September after a progressive decrease of the river outflow, showed the typical situation of a concentrated maximum turbidity zone surrounding the river mouth and only extending over the river delta.

Due to the absence of match-ups between satellite and field measurements in 2009, the SPM quantification algorithm developed and applied to MODIS data could not be fully validated. However a cross-validation was obtained between the SPM

quantification relationships established using a semi-analytical then an empirical approach, which tends to prove the validity of the algorithm. The SPM quantification relationship developed for the Mackenzie plume was proved to be similar to relationships established in turbid European estuarine waters. However it is potentially affected by variations of CDOM concentrations which significantly impact on light absorption at 555 nm and induce uncertainties on satellite-derived SPM concentrations. Nonetheless concentrations retrieved from MODIS data proved to be consistent with field observations.

3.5 Vertical dynamics of SPM in the Mackenzie River delta

Ocean colour satellite data proved to provide useful information about the extension and dynamics of the Mackenzie River plume, through the estimation of surface SPM concentrations. However, remote sensing observations also present two major limits in the scope of studying SPM dynamics in a river plume. Firstly they are limited to subsurface waters, i.e. the layer below the water surface where the solar light penetrates and is reflected towards satellite sensors. Depending on water turbidity and on the wavelength considered, this layer can be lower than 1 m and therefore no information is obtained concerning the vertical variations of SPM within the water column. Secondly such passive radiometric measurements are dependent on the level of cloud coverage, which may prevent observations to be collected during key periods associated with the export of particles from rivers to the ocean (e.g. the summer 2009 period over the Mackenzie continental shelf). Field observations are therefore necessary to provide regular measurements within the whole water column, e.g. to detect bottom and intermediate nepheloid layers.

The Malina dataset was used specifically to document the vertical distribution of SPM in the Mackenzie River delta apparently associated with a permanent maximum turbidity zone. CTD and bio-optical measurements were carried out along river transects on 13 August 2009 (west side) and 16 August 2009 (east side), at a distance greater than 50 km offshore from the river mouth (salinity of 0, water depths of 2 m (west) and 8 m

(east)). For both transects, the $b_{bp}(715)$ coefficient was used as a proxy for the SPM concentration. The water mass was well mixed and almost homogeneous in terms of temperature and salinity at the river mouth while the stratification between fresh and salted waters started 5 km offshore.

The most turbid waters were located in shallow regions of the western river mouth with almost homogeneous vertical profiles of SPM along a 10 km distance (Fig. 8). From 10 to 35 km offshore from the mouth, two turbidity layers clearly formed: a 4 m thick surface layer and a thinner but more turbid bottom layer probably associated with different kinds of SPM (fine particles at the surface and coarse aggregates close to the bottom). The maximum turbidity zone was strictly confined within the river delta up to the 10 m isobath. Offshore, the water mass remained slightly stratified with significantly lower SPM concentrations ($<5\,\mathrm{g\,m}^{-3}$).

Along the east river transect, SPM concentrations were approximately half those observed on the west side of the mouth. In terms of vertical profiles of turbidity and salinity, the water mass was rather homogeneous at the river mouth then progressively stratified to highly stratified from the river mouth to 50 km offshore (10 m isobath). With increasing distance from the mouth, the surface plume progressively declined while the bottom layer became thicker with higher SPM concentrations, most probably resulting from flocculation processes which enhanced SPM settling (Droppo et al., 1998). This assumption is supported by the observed variation trend in the shape of the attenuation coefficient spectrum ($c(\lambda) = A\lambda^{-\gamma}$, with γ the spectral slope): γ typically decreases from 1.5 within surface waters to 0.8 in the bottom layer (not shown). These variations are representative of changes in the particle size distribution along the water column, with an increasing proportion of coarse particles occurring for decreasing γ values (Boss et al., 2001).

The intensive flocculation of fine particles exported by the Mackenzie River onto the shelf has been documented to occur for water salinity varying from 0 to 4 (Droppo et al., 1998). This seems to be the case in our dataset where the SPM concentration within surface waters was observed to decrease by a factor of 7 from the river mouth

(west side) to adjacent coastal waters with salinity of 5, i.e. along a distance of 30 km (Fig. 10). As a first approximation ($R^2 =$ ⬚), a power-law function can be used to model the decrease in SPM concentration increasing water salinity. Most of the terrigenous SPM seems therefore affected by flocculation processes and settles down close to the mouth, in the delta zone. Despite these intensive flocculation processes, a significant amount of SPM appears to remain in suspension and be transported offshore, as highlighted by the observed SPM concentrations which smoothly decrease from about 10 to 1 g m^{-3} as water salinity increases from 5 to about 25 (Fig. 10). This phenomenon is apparently independent of the river outflow as observed on both west and east river transects. Variations of water salinity in the delta zone also appear as a reasonably good ($R^2 = 0.83$) indicator of the POC:SPM ratio, with ratio values close to 2 % at the river mouth (salinity ⬚) almost linearly increasing to values of about 10 % for water salinities of 20 (Fig. 10). Note this relationship is obtained when combining the Malina dataset to previous measurements carried out during as part of the Canadian Arctic Shelf Exchange Study in 2004 (Bélanger et al., 2008). These variations are representative of the complex processes occurring in the delta zone, including: (i) advection and (ii) dilution of the turbid freshwater discharged by the Mackenzie River, (iii) intensive flocculation of the predominantly-mineral terrigenous particles with biogenic organic matter.

Field measurements are therefore in agreement with satellite observations: both locate majority of the SPM on the west part of the river mouth, with a maximum turbidity zone confined in the river delta (water depth <10 m). The vertical homogeneity of water turbidity results from the high river outflow, as up to 80 % of the Mackenzie freshwater discharge into the Beaufort Sea occurs through the west mouth. During the sampling period, the outflow through the east river mouth was too low to homogeneously maintain particles in suspension, so that stratification of turbidity rapidly occurred.

3.6 Estimation of SPM and POC fluxes at the river mouth

We finally attempt to estimate the fluxes of SPM and POC at the mouth of the Mackenzie River. For that we use (i) the freshwater discharge (monthly averages) measured by the Canadian Water Office, (ii) SPM concentrations retrieved from MODIS satellite data and (iii) POC:SPM ratio values documented based on field observations (river transects) during the Malina campaign. Estimations are therefore limited to the 2009, 2010 and 2011 summer periods (June to September). Available satellite observations are averaged within each month to produce monthly averages of SPM concentrations at the river mouth (i.e. within the pixels containing the two most upstream stations sampled along the river transects). It implies that the averaged SPM concentration obtained is more or less representative of the monthly averages depending on the number of satellite observations available. The SPM concentration retrieved from satellite data is assumed to be equal to the mean SPM concentration within the water column at the river mouth where water depths are respectively 2 m (west side) and 8 m (east side). This assumption is supported by our field optical measurements (see Figs. 8 and 9). The POC:SPM ratio at the river mouth is set to 2 %, based on our field dataset.

MODIS-Aqua satellite images providing cloud-free views of the whole Mackenzie River mouth were processed for the 2009, 2010 and 2011 summer periods. It allowed the estimation of the monthly-averaged SPM concentration in (i) July and August 2009 (3 and 2 MODIS-Aqua images, respectively), (ii) June, August and September 2010 (2, 1 and 2 images, respectively) and (iii) June, August and September 2011 (3, 3 and 2 images, respectively). The resulting monthly-averaged SPM concentrations were: 245 and 145 g m^{-3} (2009), 315, 175 and 145 g m^{-3} (2010), 345, 145 and 130 g m^{-3} (2011). These values were multiplied by the volume (in m^3) of freshwater discharged each month to obtain an estimation of the SPM fluxes: (i) 18.4 × ⬚ tons in July and August 2009, (ii) 23.1 × 10^6 tons in June, August and September 2010 and (iii) 29.2 × 10^6 tons in June, August and September 2011. Assuming a constant POC:SPM ratio of 2 % at the river mouth during these periods, the corresponding POC fluxes are: (i) 0.37 × 10^6

tons in July and August 2009, (ii) 0.46×10^6 tons in June, August and September 2010 and (iii) 0.58×10^6 tons in June, August and September 2011.

These monthly fluxes can be compared to previous rough estimates of SPM and POC delivered annually by the Mackenzie River to the delta: 127×10^6 tons and 2.1×10^6 tons, respectively (McDonald et al., 1998 and references therein). Our estimates are in the good order of magnitude but are lower than expected considering that most of the freshwater and SPM are discharged between May and September. First, our SPM algorithm still requires a validation based on match-ups with field measurements at the river mouth. Second, the monthly-averaged SPM concentrations estimated from ocean colour remote sensing data depend on the number of available cloud-free satellite images; this number can significantly increase by using MERIS and MODIS-Terra satellite observations in addition to MODIS-Aqua. Third, the highest SPM concentrations at the Mackenzie River mouth are certainly found in May and June during the breaking-up of the stamukhi, periods during which few cloud-free satellite observations were available in 2009, 2010 and 2011. This may partly explain the rather low SPM fluxes estimated based on remote sensing data in the present study. Moreover, previous estimates were based on field measurements made in the Mackenzie River, i.e. upstream the river delta, while our remote sensing observations concerned the mouth of the Mackenzie River, i.e. the exact limit between the river and adjacent coastal waters. The trapping of SPM in the delta zone should be taken into account when comparing solid fluxes measured in a river station and fluxes actually exported to the coastal ocean (e.g. Seitzinger et al., 2005; Doxaran et al., 2009), which may promote the preferential use of remote sensing techniques.

4 Conclusions

This study first allowed documentation of the organic carbon content of particles in suspension in the Mackenzie River delta, turbid plume and adjacent Beaufort Sea waters during the summer 2009. The content was shown to vary from one extreme to another,

5231

i.e. from the mineral-rich particles at the river mouth (POC:SPM ratio of 2 % on average) to organic-rich particles away from the river plume (POC:SPM ratio in the range 10–45 %). The river plume waters appeared as a complex transition zone with mixed mineral and organic particles and a POC:SPM ratio typically increasing with decreasing SPM concentration. An important implication is that POC concentrations can be accurately estimated at least at the river mouth from SPM concentration measurements (in situ or remotely sensed).

Regional proxies were identified to estimate SPM concentrations in the Mackenzie River delta and turbid plume from bio-optical measurements, namely based on the attenuation and particulate backscattering coefficients. Moreover, a robust quantification relationship was developed to estimate SPM concentrations from remote sensing reflectance (R_{rs}) measurements (i.e. either from field or atmospherically-corrected ocean colour satellite data). This relationship was established using a semi-analytical approach based on the measured SPM mass-specific inherent optical properties then validated using a fully-empirical approach used to relate R_{rs} and SPM concentration field measurements. The results obtained proved to be similar to those previously obtained in sediment-dominated European estuaries (Doxaran et al., 2006). The regional relationship established in the Mackenzie River plume was proved to be robust but still significantly affected by variations in CDOM concentrations.

The application of this relationship to ocean colour satellite data requires the accurate retrieval of the R_{rs} signal in visible (around 560 nm) and near-infrared (around 780 nm) spectral bands. It was tested on a selection of cloud-free MODIS-Aqua satellite data recorded in 2009, 2010 and 2011. The near-infrared (two bands) atmospheric correction provided satisfactory results, in terms of R_{rs} retrieval, in the moderately turbid waters of the Mackenzie River plume. As a result, the surface SPM concentrations retrieved from MODIS data were within the expected range and allowed analysis of the seasonal to multi-annual dynamics of SPM. A permanent maximum turbidity zone was identified in the river delta (up to the 10 m isobath) while the offshore extension of the

5232

plume (predominantly westwards or northwards) was observed to closely respond to variations in the Mackenzie freshwater discharge.

The location of the maximum turbidity zone in the river delta was confirmed by field measurements which also allowed detection of the presence of mineral-rich particles within surface waters of the Beaufort Sea, up to 300 km offshore. Moreover, SPM concentrations at the river mouth were observed to exhibit weak vertical variations along the water column, implying that ocean colour remote sensing data can be used to provide new estimates of SPM and POC fluxes exported by the Mackenzie River into the Beaufort Sea. The fluxes estimated in this study as part of a preliminary exercise proved to be in the good range but further work (i.e. field and satellite observations) is necessary to quantify the said fluxes during the spring (May–June) period.

Additional field measurements are required to assess the robustness of the optical proxies identified in this study, and the validity of the SPM quantification algorithm developed for ocean colour remote sensing. In an optimal scenario, in situ field data would be acquired coincidentally with satellite imagery (a so called match-up). The next step will be the routine application of the developed quantification algorithm to MODIS and MERIS satellite data for operational monitoring of the SPM and POC fluxes delivered by the Mackenzie and other major rivers to the Arctic Ocean.

5233

The publication of this article is financed by CNRS-INSU.

References

Antoine, D., Morel, A., Leymarie, E., Houyou, A., Gentili, B., Victori, S., Buis, J.-P., Buis, N., Meunier, S., Canini, M., Crozel, D., Fougnie, B., and Henry, P.: Underwater radiance distributions measured with miniaturized multispectral radiance cameras, J. Atm. Ocea. Tech., submitted, 2012.

Babin, M., Stramski, D., Ferrari, G. M., Claustre, H., Bricaud, A., Obolensky, G., and Hoepffner, N.: Variations in the light absorption coefficients of phytoplankton, non-algal particles, and dissolved organic matter in coastal waters around Europe, J. Geophys. Res., 108, C7, 3211, doi:10.1029/2001JC000882, 2003a.

Babin, M., Morel, A., Fournier-Sicre, V., Fell, F., and Stramski, D.: Light scattering properties of marine particles in coastal and oceanic waters as related to the particle mass concentration, Limnol. Oceanogr., 48, 843–859, 2003b.

Bélanger, S., Babin, M., and Larouche, P.: An empirical ocean color algorithm for estimating the contribution of chromophoric dissolved organic matter to total light absorption in optically complex waters, J. Geophys. Res., 113, C04027, doi:10.1029/2007JC004436, 2008.

Boss, E. and Pegau, W. S.: Relationship of light scattering at an angle in the backward direction to the backscattering coefficient, Appl. Opt., 40, 5503–5507, 2001.

Boss, E., Pegau, W. S., Gardner, W. D., Zaneveld, J. R. V., Barnard, A. H., Twardowski, M. S., Chang, G. C., and Dickey, T. D.: Spectral particulate attenuation and particulate size distribution in the boundary layer of a continental shelf, J. Geophys. Res., 106, 9509–9516, 2001.

5234

Bricaud, A. and Stramski, D.: Spectral absorption coefficients of living phytoplankton and non-algal biogenous matter: A comparison between the Peru upwelling area and the Sargasso Sea, Limnol. Oceanogr., 35, 562–582, 1990.

Copin-Montégut, G.: Matière en suspension dans les eaux de mer: répartition, composition chimique, origine et e'volution, Laboratoire de Physique et Chimie Marines. Thesis, Université Pierre et Marie Curie, 173, 1980.

Carmack, E. C. and Macdonald, W. R.: Oceanography of the Canadian Shelf of the Beaufort Sea: A Setting for Marine Life, Arctic, 55, 29–45, 2002.

Doxaran, D., Froidefond, J. M., Lavender, S. J., and Castaing, P.: Spectral signature of highly turbid waters. Application with SPOT data to quantify suspended particulate matter concentrations, Remote Sens. Environ., 81, 149–161, 2002.

Doxaran, D., Froidefond, J. M., and Castaing, P.: Remote sensing reflectance of turbid sediment- dominated waters. Reduction of sediment type variations and changing illumination conditions effects using reflectance ratios, Appl. Opt., 42, 2623–2634, 2003.

Doxaran, D., Cherukuru, R. C. N., and Lavender, S. J.: Inherent and apparent optical properties of turbid estuarine waters: measurements, modelling and application to remote sensing, Appl. Opt., 45, 2310–2324, 2006.

Doxaran, D., Froidefond, J. M., Castaing, P., and Babin, M.: Dynamics of the turbidity maximum zone in a macrotidal estuary (the Gironde, France): Observations from field and MODIS satellite data, Estuar. Coast. Shelf Sc., 81, 321–332, 2009.

Droppo, I. G., Jeffries, D., Jaskot, C., and Backus, S.: The prevalence of freshwater flocculation in cold regions: A case study from the Mackenzie River Delta, Northwest Territories, Canada, Arctic, 51, 155–164, 1998.

Frey, K. E. and McClelland, J. W.: Impacts of permafrost degradation on arctic river biogeochemistry, Hydrol. Proces., 23, 1, 169–182, 2009.

Gordon, H. R., Brown, O. B., and Jacobs, M. M.: Computed relations between the inherent and apparent optical properties of a flat homogeneous ocean, Appl. Opt., 14, 417–427, 1975.

Hedges, J. I., Keil, R. G., and Benner, R.: What happens to terrestrial organic matter in the ocean? Org. Biogeochem., 27, 195–212, 1997.

Kishino, M., Takahashi, M., Okami, N., and Ichimura, S.: Estimation of the spectral absorption coefficients of phytoplankton in the sea, Bull. Mar. Sci., 37, 634–642, 1985.

Kou, L., Labrie, D., and Chylek, P.: Refractive indices of water and ice in the 0.65- to 2.5-μm spectral range, Appl. Opt., 32, 3531–3540, 1993.

Langford, V. S., McKinley, A. J., and Quickenden, T. I.: Temperature dependence of the visible-near-infrared absorption spectrum of liquid water, J. Phys. Chem. A, 105, 8916–8921, 2001.

Loisel, H. and Morel, A.: Non-isotropy of the upward-radiance field in typical coastal case 2 waters, Int. J. Remote Sens., 22, 275–295, 2001.

Macdonald, R. W., Paton, D. W., Carmack, E. C., and Omstedt, A.: The freshwater budget and under-ice spreading of Mackenzie River water in the Canadian Beaufort Sea based on salinity and $^{18}O/^{16}O$ measurements in water and ice, J. Geophys. Res., 100, 895–919, 1995.

Macdonald, R. W., Solomon, S. M., Cranston, R. E., Welch, H. E., Yunker, M. B., and Gobeil, C.: A sediment and organic carbon budget for the Canadian Beaufort shelf, Mar. Geol., 144, 255–273, 1998.

Macdonald, R. W., McLaughlin, F. A., and Carmack, E. C.: Freshwater and its sources during the SHEBA drift in the Canada Basin of the Arctic Ocean, Deep-Sea Res., 49, 1769–1785, 2002.

Matsuoka, A., Bricaud, A., Benner, R., Para, J., Sempéré, R., Prieur, L., Bélanger, S., and Babin, M.: Tracing the transport of colored dissolved organic matter in water masses of the Southern Beaufort Sea: relationship with hydrographic characteristics, Biogeosciences, 9, 925–940, doi:10.5194/bg-9-925-2012, 2012.

McKee, D., Chami, M., Brown, I., Calzado, V. S., Doxaran, D., and Cunningham, A.: Role of measurement uncertainties in observed variability in the spectral backscattering ratio: a case study in mineral-rich coastal waters, Appl. Opt., 48, 4663–4675, 2009.

Mobley, C. D.: Light and Water: Radiative Transfer in Natural Waters, Academic, San Diego, Calif., 1994.

McClelland, J. W., Holmes, R. M., Dunton, K. H., and Macdonald, R. W.: The Arctic Ocean Estuary, Estuar. Coasts, 35, 2, 353–368, doi:10.1007/s12237-010-9357-3, 2012.

Mobley, C. D.: Estimation of the remote-sensing reflectance from above-surface measurements, Appl. Opt., 38, 7442–7455, 1999.

Morel, A.: Optical properties of pure water and pure seawater, in: Optical aspects of oceanography, edited by: Jerlov, E. and Steeman Nielsen, Academic, 1–24, 1974.

Morel, A. and Prieur, L.: Analysis of variations in ocean color, Limnol. Oceanogr., 22, 709–722, 1977.

Morrow, J. H., Booth, C. R., Lind, R. N., and Hooker, S. B.: "The Compact-Optical Profiling System (C-OPS)," in: Advances in Measuring the Apparent Optical Properties (AOPs) of Optically Complex Waters, edited by: Morrow, J. H., Hooker, S. B., Booth, C. R., Bernhard,

G., Lind, R. N., and Brown, J. W., NASA Tech. Memo. 2010–215856, NASA Goddard Space Flight Center, Greenbelt, Maryland, 42–50, 2010.

Neukermans, G., Loisel, H., Mériaux, X., Astoreca, R., and McKee, D.: In situ variability of mass-specific beam attenuation and backscattering of marine particles with respect to particle size, density, and composition, Limnol. Oceanogr., 57, 124–144, doi:10.4319/lo.2011.57.1.0124, 2012.

O'Brien, M. C., Macdonald, R. W., Melling, H., and Iseki, K.: Particle fluxes and geochemistry on the Canadian Beaufort shelf: implications for sediment transport and deposition, Cont. Shelf Res., 26, 41–81, 2006.

Park, Y. and Ruddick, K.: Model of remote-sensing reflectance including bidirectional effects for case 1 and case 2 waters, Appl. Opt., 44, 1236–1249, 2005.

Peterson, B. J., Holmes, R.M., McClelland, J. W., Vörösmarty, C. J., Lammers, R. B., Shiklomanov, A. I., Shiklomanov, I. A., and Rahmstorf, S.: Increasing river discharge to the Arctic Ocean, Science, 298, 2171–2173, 2002.

Rachold, V. H., Eicken, V. V., Gordeev, M. N., Grigoriev, H. W., Hubberten, A. P., Lisitzin, V., Shevchenko, P., and Schirrmeister, L.: Modern terrigenous organic carbon input to the Arctic Ocean, in: The organic carbon cycle in the Arctic Ocean, edited by: Stein, R. and MacDonald, R. W., Springer, New-York, 33–54, 2004.

Roesler, C. S.: Theoretical and experimental approaches to improve the accuracy of particulate absorption coefficients from the Quantitative Filter Technique, Limnol. Oceanogr., 43, 1649–1660, 1998.

Röttgers, R. and Gehnke, S.: Light absorption by natural aquatic particles in the near-infrared (700–900 nm) spectral region, Appl. Opt., 51, 1336–1351, 2012.

Schlunz, B. and Schneider, R. R.: Transport of terrestrial organic carbon to the oceans by rivers: re-estimating flux and burial rates, Int. J. Earth Sciences, 88, 599–606, 2000.

Seitzinger, S. P., Harrison, J. A., Dumont, E., Beusen, A. H. W., and Bouwman, A. F.: Sources and delivery of carbon, nitrogen, and phosphorus to the coastal zone: An overview of Global Nutrient Export from Watersheds (NEWS) models and their application, Global Biogeochem. Cy., 19, GB4S01, doi:10.1029/2005GB002606, 2005.

Sullivan, J. M., Twardowski, M. S., Zaneveld, J. R. V., Moore, C. M., Barnard, A. H., Donaghay, P. L., and Rhoades, B.: Hyperspectral temperature and salt dependence of absorption by water and heavy water in the 450–750 nm spectral range, Appl. Opt., 45, 5294–5309, 2006.

Twardowski, M. S., Boss, E., Macdonald, J. B., Pegau, W. S., Barnard, A. H., and Zaneveld, J. R. V.: A model for estimating bulk refractive index from the optical backscattering ratio and the implications for understanding particle composition in case I and case II waters, J. Geophys. Res., 106, 14129–14142, doi:10.1029/2000JC000404, 2001.

Van Der Linde, D. W.: Protocol for determination of total suspended matter in oceans and coastal zones, JRC Technical Note I., 98, 182, 1998.

Van Raaphorst, W. and Malschaert, J. F. P.: Ammonium adsorption in superficial North Sea sediments, Cont. Shelf Res., 16, 1415–1435, 1996.

Wang, M. and Shi, W.: The NIR-SWIR combined atmospheric correction approach for MODIS ocean color data processing, Opt. Express, 15, 15722–15733, 2007.

Wetlabs ECO BB User's Guide, Revision AC, Wetlabs Inc, 2007.

Wetlabs Absorption and Attenuation Meter (ac-9) User's Guide, Revision S, Wetlabs Inc, 2008.

Yunker, M. B., Macdonald, R. W., Cretney, W. J., Fowler, B. R., and McLaughlin, F. A.: Alkane, terpene, and polycyclic aromatic hydrocarbon geochemistry of the Mackenzie River and shelf: riverine contributions to Beaufort Sea coastal sediments, Geochim. Cosmochim. Ac., 57, 3041–3061, 1993.

Zaneveld, J. R. V., Kitchen, J. C., and Moore, C.: The scattering error correction of reflecting-tube absorption meters, Ocean Optics XII. Soc. Photo-Optical Instrum. Eng. (SPIE), 44–55, 1994.
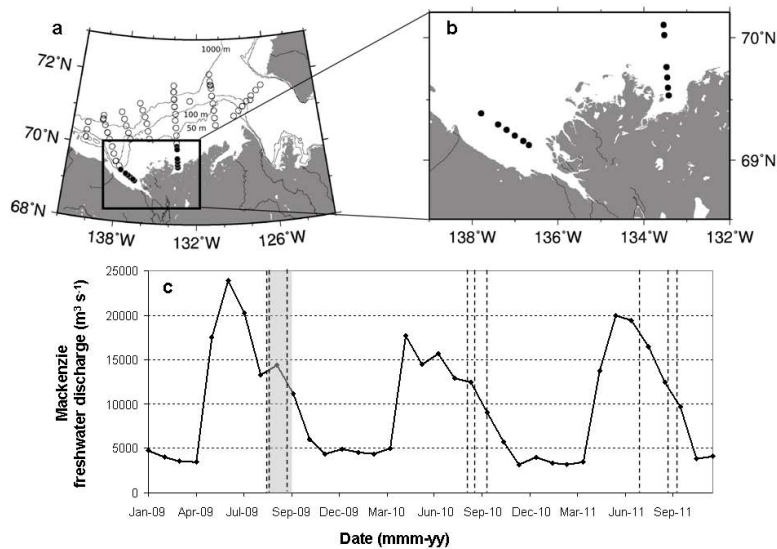
Fig. 1. Study area and sampling stations: whole study area **(a)** and river transects **(b)**. Sampling stations (white points) and river transects stations (black points). Mackenzie River freshwater discharge in 2009, 2010 and 2011 **(c)** with the Malina field experiment period (in grey) and dates of the selected MODIS satellite images (dashed lines).
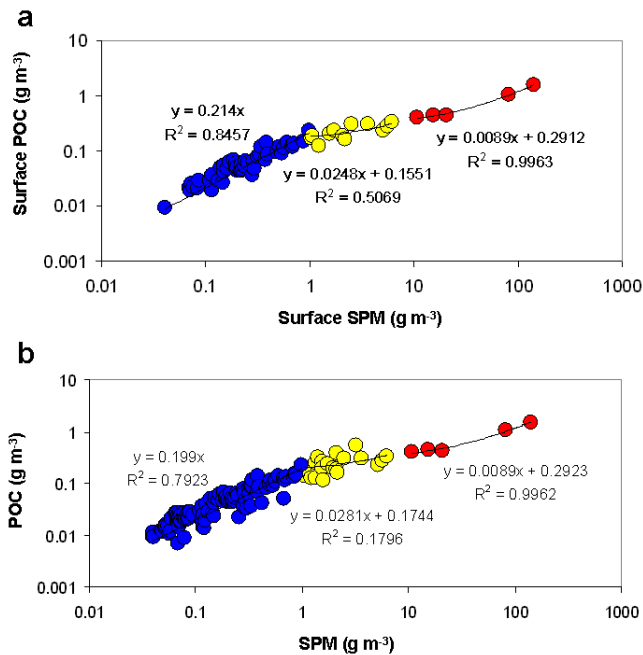
5239

Fig. 2. Relationship between the POC and SPM concentrations in the Mackenzie continental shelf: **(a)** within surface waters (0–4 m depth) and **(b)** within the water column (0–150 m depth). The following three ranges of SPM concentrations are distinguished: 0.02–1 g m^{-3} (blue); 1–10 g m^{-3} (red) and 10–200 g m^{-3} (red).

5240
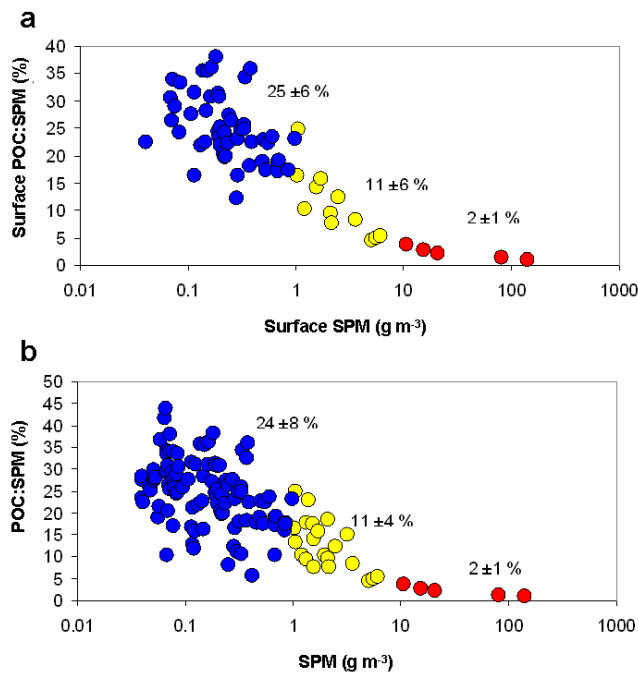
Fig. 3. Variations of the POC:SPM ratio (in %) in the Mackenzie continental shelf as a function of the SPM concentration: **(a)** within surface waters (0–4 m depth) and **(b)** within the water column (0–150 m depth). The following three ranges of SPM concentrations are distinguished: $0.02–1\,\mathrm{g\,m}^{-3}$ (blue); $1–10\,\mathrm{g\,m}^{-3}$ (red) and $10–200\,\mathrm{g\,m}^{-3}$ (red).
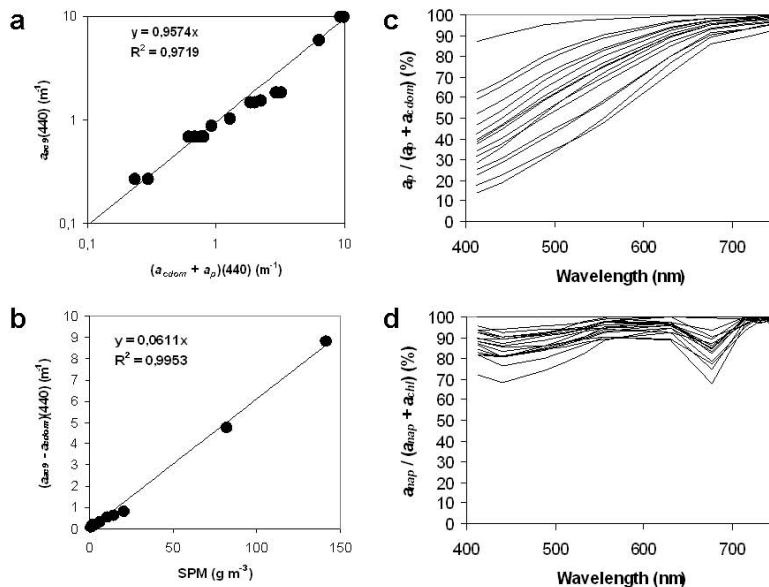
Fig. 4. Light absorption by SPM along the two river transects: **(a)** Consistency between the light absorption measured with the ac-9 sensors (referenced to pure water) and light absorption by SPM (spectrophotometric measurements on particles retained on glass-fibre filters) plus light absorption by CDOM ((Ultrapath measurements), at 440 nm; **(b)** Light absorption measured with the ac-9 sensors as a function of the SPM concentration; **(c)** Spectral contribution of particulate light absorption to particulate and CDOM light absorption; **(d)** Spectral contribution of light absorption by NAP to particulate light absorption.
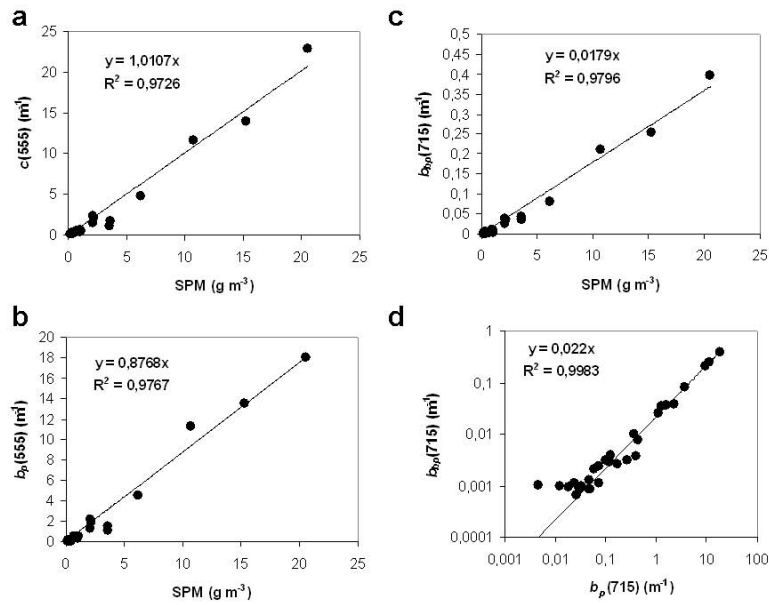
Fig. 5. Particulate light attenuation **(a)**, scattering **(b)** and backscattering **(c)** as a function of the SPM concentration. Results are presented at 555 nm (attenuation and scattering) and 715 nm (backscattering). Relationship between particulate light scattering and backscattering at 715 nm **(d)**.
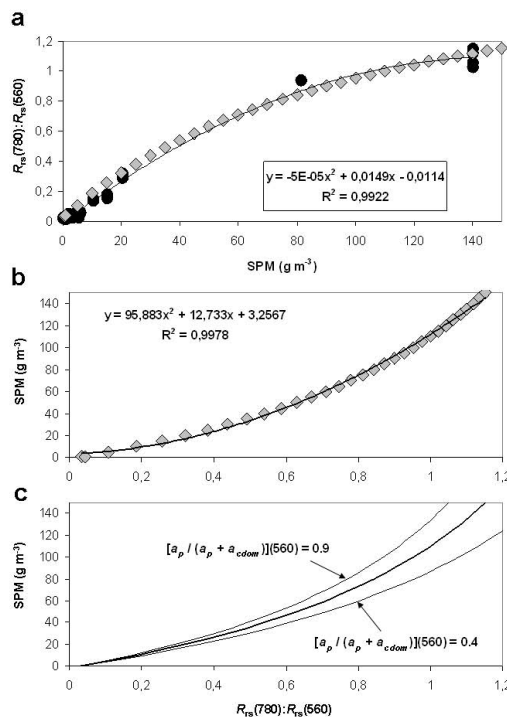
Fig. 6. Relationship between the $R_{rs}(780){:}R_{rs}(560)$ ratio and SPM concentration along the two river transects. **(a)** Empirical relationship (black points) with the associated best second order polynomial fit and semi-analytical relationship (grey points). **(b)** Inverse semi-analytical relationship giving the SPM concentration from the $R_{rs}(780){:}R_{rs}(560)$ ratio. **(c)** Influence of the CDOM contribution at 560 nm (grey lines).
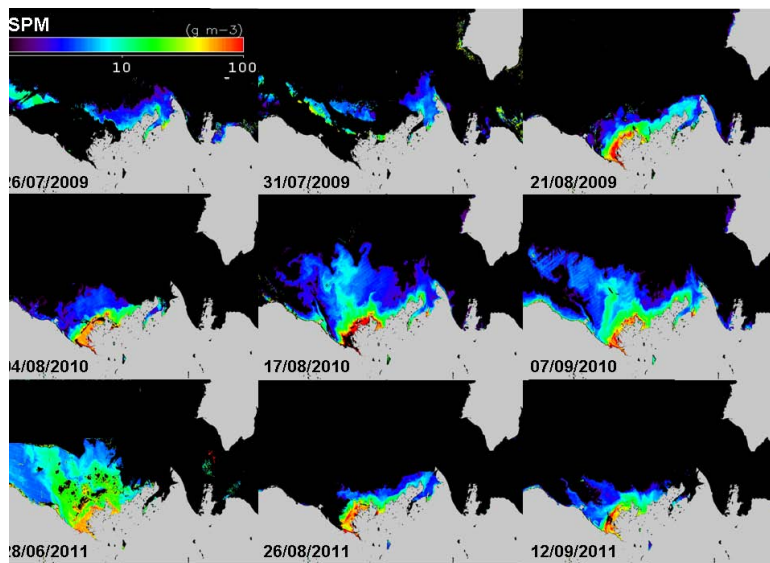
Fig. 7. Maps of SPM concentrations retrieved from selected MODIS-Aqua satellite data recorded in 2009 (top), 2010 (middle) and 2011 (bottom).
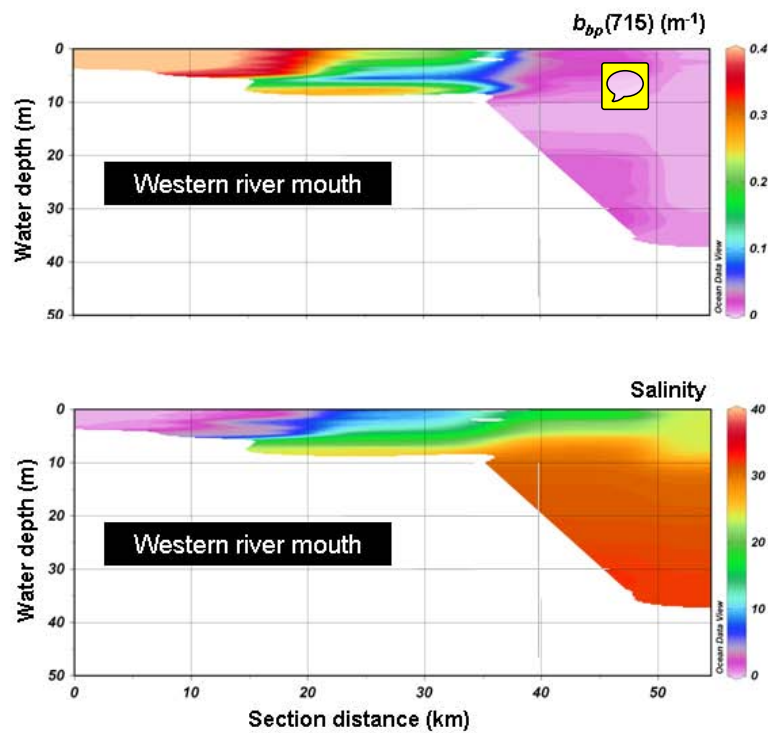
Fig. 8. Spatial variations of $b_{bp}(715)$, in m^{-1}, (a proxy for the SPM concentration, and water salinity along the Mackenzie River mouth (west side). Measurements were carried out on the 13 August 2009.
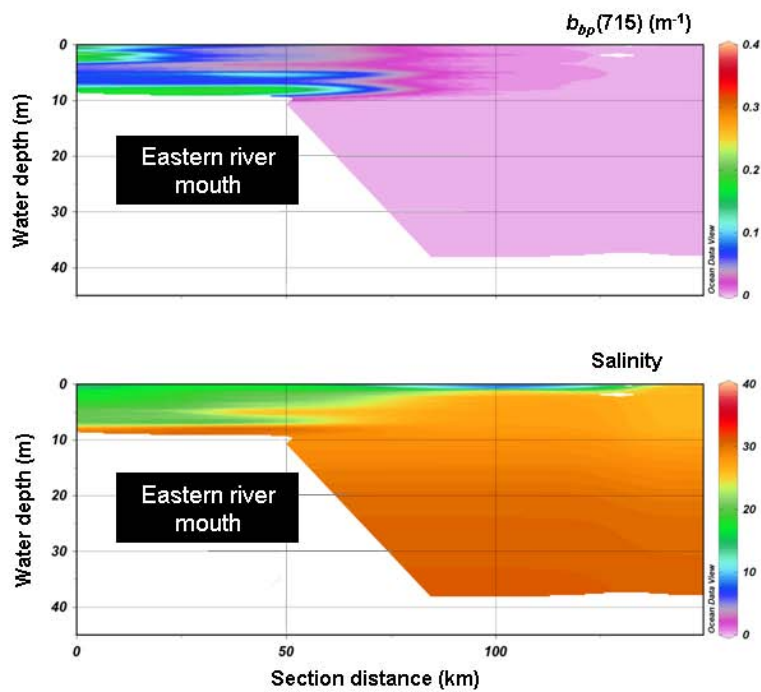
Fig. 9. Spatial variations of $b_{bp}(715)$, in m^{-1}, (a proxy for the SPM concentration, and water salinity along the Mackenzie River mouth (east side). Measurements were carried out on the 16 August 2009.
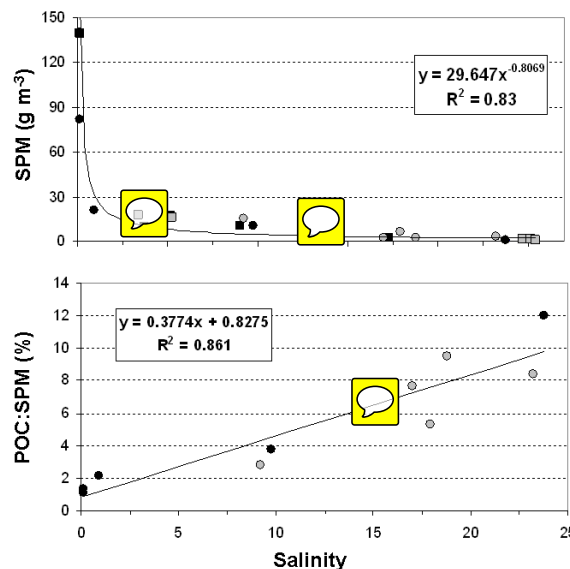
5247

Fig. 10. Observed variations of the SPM concentration (top) and POC:SPM ratio (bottom) as a function of water salinity. Only stations along the two river transects where the water salinity, SPM and POC concentrations were measured simultaneously are reported. Black and grey circles respectively represent the west and east river transects. For comparisons measurements of salinity and SPM concentrations carried out along the same river transects during the Canadian Arctic Shelf Exchange Study in June and July 2004 (see Bélanger et al. (2008) for exact sampling locations) (black and grey squares, respectively for the west and east river transects) are included. The power-law regression between SPM and salinity is obtained when considering the Malina and CASES measurements.

5248